IEEE Access
Multidisciplinary | Rapid Review | Open Access Journal

Received November 12, 2017, accepted December 14, 2017, date of publication January 1, 2018,
date of current version February 28, 2018.

*Digital Object Identifier 10.1109/ACCESS.2017.2788941*

# Multi-Objective Optimal Control Allocation for an Over-Actuated Electric Vehicle

**HOUHUA JING, FENGJIAO JIA, AND ZHIYUAN LIU, (Member, IEEE)**
Department of Control Science and Engineering, Harbin Institute of Technology, Harbin 150001, China

Corresponding author: Houhua Jing (jinghouhua@hit.edu.cn)

This work was supported in part by the National Natural Science Foundation of China under Grant 61403105, and in part by the China Automobile Industry Innovation and Development Joint Fund under Grant U1564207.

**ABSTRACT** The in-wheel-motor-driven electric vehicle is a typical over-actuated system. The actuation flexibility can be utilized to improve operational efficiency and enhance vehicle motion control performance by allocating different torques to four wheels. Various control objectives are emphasized for different working conditions. To trade off energy optimization and driving stability in actual complicated conditions, a unified control allocation law composed of two-step optimization is developed. A pre-allocation law is carried out for energy efficiency optimization with the assumption that no wheel is skidding or slipping, and a control reallocation law is performed using model predictive control to avoid the vehicle from unstability and to enhance the driving performance. Simulation tests are carried out via a professional vehicle dynamics simulating software veDYNA. The controller is verified to improve energy recovery in routine stable driving conditions and also to dynamically modify torques to ensure the vehicle stability on mu-split and low-adhesion road in extreme conditions.

**INDEX TERMS** Over-actuated electric vehicle, multi-objective optimal, control allocation, model predictive control.

## I. INTRODUCTION

Electric vehicle (EV) has attracted increasing attention from both industrial and academic communities recently. The motor has high efficiency and fast response, which is helpful to improve energy saving and vehicle stability, especially for the electric vehicle with four independently actuated in-wheel motors [1], [2]. One highlighted advantage of the in-wheel-motor-driven electric vehicle is higher control flexibility, i.e., the torque of each in-wheel motor can be independently and precisely controlled. The actuation flexibilities together with the motors' fast and precise torque responses can enhance vehicle motion control performance, e.g., in traction control system [3], [4], anti-lock braking system [5], [6], and yaw stability control system [7], [8]. Moreover, the actuation flexibility can also be utilized for improving the operational efficiency by allocating different torques to the four wheels with respect to the desired total torque and motor efficiency.

As well known, driving distance is the choke point of electric vehicles, so it is significant to research on how to improve the energy efficiency [9]. For instance, a range extension control system was proposed to minimize resistance with driving force distribution ratio between front and rear wheels in [10], and an energy optimal control approach was developed by minimizing actuator losses and power consumption for driving along a pre-calculated trajectory in [11]. For a general optimization problem, minimum actuation magnitudes for actuators is always used as cost function, but it does not necessarily lead to minimum power consumption due to actuators' efficiency characteristics. The motor efficiency is highly dependent on the working speed or torque, and the efficiency curves are not strictly concave or convex. Thereby, it will come to a non-convex optimization problem by explicitly incorporating the efficiency functions. A numerical method was proposed in [12], and the results showed good potentials for improving the operational energy efficiency. Further, by fitting the motor efficiency with polynomial, various non-convex optimization algorithms were developed in order to simultaneously achieve energy optimization as well as desired vehicle dynamics control in [13]–[15]. Also, a real-time torque distribution strategy was determined by particle swarm optimization theory in [16]. Additionally, more characteristics such as clutch control were also taken into account for complicated system [17], [18]. The aforementioned research contributed to energy-saving, but the application was limited on

condition that no wheel was skidding or slipping. The methods are not suitable for urgent operations or on low adhesion roads, because the tire friction saturation is not taken into account.

Due to the variety and complexity of driver operation and road condition, not only the energy efficiency but also the tire friction saturation should be considered for control allocation. Therefore, it comes to a constrained optimal problem or a multi-objective optimal problem. Model predictive control is an effective solution and widely used in electric vehicle control allocation in recent years [19]. References [20]–[22] researched on real-time model predictive control allocation algorithms for the over-actuated electric vehicles, in which the tire friction saturation was formulated as soft constraints on wheel slip or tire forces. The vehicle longitudinal force and yaw moment were pre-distributed into wheel torques based on wheel loads, and then wheel torques were re-distributed by considering the wheel dynamics or actuator dynamics by using model predictive control method. In [23], a model predictive regenerative braking controller was proposed, where the energy-saving objective was accomplished by including in the cost function the additional penalty term on the motor-to-battery regenerative braking power, while the safety objective was formulated as hard constraints on the wheel slip ratios. Initial plane gridding was applied for better solution of the constrained nonlinear optimization problem. Reference [24] proposed a model predictive control allocation approach to solve the torque blending problem of the hybrid braking system, and provided a detailed comparison between the proposed method and two other allocation solutions. These model predictive control laws paid more attention to the optimal control allocation constrained by the tire forces, while the in-wheel motor efficiency curves were ignored. As mentioned above, minimum actuation magnitudes for actuators does not necessarily lead to minimum power consumption due to actuators' efficiency characteristics.

To sum up, a considerate control method should take into account of actuators' efficiency as well as the tire forces constraints. However, the existing research focused on either the energy optimization or the stability control, but not considering both sides. Due to the complicated condition and various operations in practice, the two distinct controllers would be actuated alternately. The controller switching might cause a drastic change in control input or other potential troubles, and a smoothly transition cannot be guaranteed owing to lack of supervision. Besides, the separated two modes cannot handle properly the transitional condition between the two cases. The main objective of this paper is to design a unified control allocation law to deal with the various requirements in more complicated cases, i.e., to improve the energy recovery if all wheels work stably, to keep stability if the vehicle tends to unstable, and also to enhance the vehicle driving or braking performance by dynamic allocation if some individual wheel is skidding or slipping. In order to simplify problem and reduce computational load, the constrained optimization problem is decomposed into two-step optimal problems to deal with the energy saving and the vehicle stability objectives.

The rest of this paper is organized as follows. In section II, the over-actuated electric vehicle model is presented. Then the two-step optimal controller is developed in Section III, including an off-line pre-calculated control law to optimize energy efficiency, and a dynamic control allocation modification to enhance vehicle stability and performance. In section IV, a professional simulator veDYNA is utilized for different vehicle maneuvers in order to verify improvements on both economy and safety.

## II. SYSTEM OVERVIEW AND MODELING

### A. VEHICLE STRUCTURE

In our experiment vehicle, the in-wheel motor is a permanent magnet synchronous motor and outputs torque via a fix transmission gear. Both the motor and the gear are regarded as a whole actuating module, whose output torque is $T_{\mathrm{m}i}$ and rotational speed is $\omega_i$. For braking operation, the motor will work as a generator and output regenerative braking torque [25]. The regenerative braking is limited and cannot be performed for low speed, so an electro-hydraulic braking system is applied to provide adequate braking torque [26], [27], and the hydraulic braking torque of each wheel can also be regulated independently [28]. Hence, the in-wheel-motor-driven electric vehicle is a typical over-actuated system, i.e., four motor torques for driving operation or eight braking torques for braking operation.

### B. VEHICLE DYNAMICS MODEL

As the energy-efficient performance and tire friction saturation are most concerned in this study, the simplified vehicle longitudinal dynamics is used, with five degrees of freedom for vehicle longitudinal motion and four wheels' rotation. A single wheel dynamics model is illustrated in Figure 1.

The equations of vehicle dynamics in longitudinal and rotational directions can be expressed as

$$\begin{cases} M\dot{v} = \Sigma F_{\mathrm{x}i} \\ J_{\mathrm{w}}\dot{\omega}_i = T_{\mathrm{m}i} - T_{\mathrm{h}i} - rF_{\mathrm{x}i} \end{cases} \tag{1}$$

Wheel slip ratio is introduced to describe the tire friction and the wheel dynamics, which is defined as

$$\lambda_i = \frac{r\omega_i - v}{v} \times 100\% \tag{2}$$

The tire force $F_{\mathrm{x}i}$ is related to $F_{\mathrm{z}i}$ and $\lambda_i$ [29]. In this paper, the Dugoff model is used and written as $F_{\mathrm{x}i} = f(F_{\mathrm{z}i}, \lambda_i)$ for short. Then, a simplified wheel slip dynamics equation can be obtained [30]

$$\dot{\lambda_i} = -\frac{r^2}{vJ_{\mathrm{w}}} f(F_{\mathrm{z}i}, \lambda_i) + \frac{r}{vJ_{\mathrm{w}}} T_{\mathrm{h}i} - \frac{r}{vJ_{\mathrm{w}}} T_{\mathrm{m}i} \tag{3}$$

As shown in Figure 2, the $F_{\mathrm{x}i} - \lambda_i$ curve is highly nonlinear. For most driving cases, the system works within the linear region. $\omega_i \approx v/r$ and $F_{\mathrm{x}i} \approx T_{\mathrm{m}i}/r$ hold and the vehicle is

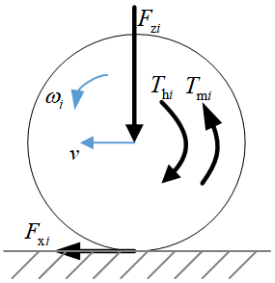


**FIGURE 1.** Single wheel model.

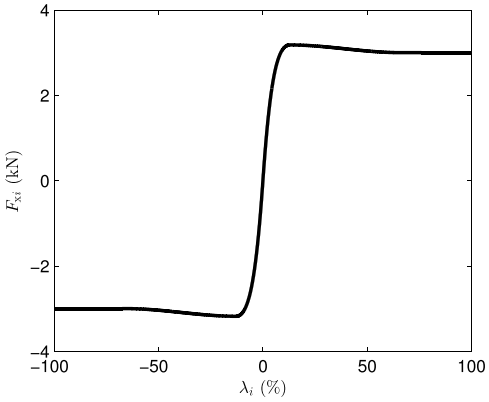


**FIGURE 2.** Relation between $F_{xi}$ and $\lambda_i$.

in a stable status. However, for an excessive driving torque $T_{mi}$, $F_{xi}$ reaches its limit. Then the system will transit to the nonlinear region and lead to an unstable behavior. That's why researchers always try to restrict $\lambda_i$ within the linear region. Similar principle holds for braking operation. Accordingly, the model can be simplified when the tire force can balance the wheel driving/braking torque, while the wheel dynamics as well as the slip ratio limit must be taken into account if the tire force gets saturated.

## III. MULTI-OBJECTIVE OPTIMAL CONTROL ALLOCATION

As shown in Figure 3, the vehicle is a human-in-the-loop system, and a hierarchical approach is beneficial for modularization and reducing complexity. Firstly, the driver determines the vehicle longitudinal force. Then a control allocation law is needed to calculate the motor torque and hydraulic torque (when braking) of each wheel. Finally, the desired wheel torques are put into effect by motor control unit or hydraulic control unit. In this work, we focus on the research of control allocation.

Both energy and stability should be considered as the main objectives for driving or braking control of an electric vehicle, so it leads to a multi-objective optimal problem. But it is challenging to solve on-line to deal with the two issues together, because the motor efficiency is highly nonlinear and the wheel slip ratios must be constrained. Thereby, a two-step optimal control allocation is developed in this paper: Firstly, a pre-allocation is carried out for energy efficiency optimization with the assumption that no wheel is skidding or slipping, called EECA for short; Then, with the pre-allocation as a reference, a control modification could be performed by reallocation to avoid the wheels from skidding or locking, called MPCA for short. In this way, not only the energy-saving objective can be achieved in most cases, but also the vehicle stability can be kept when facing a potential risk.

### A. ENERGY EFFICIENCY CONTROL ALLOCATION (EECA)

EECA is designed for the energy efficiency optimization, with the assumption that no wheel is skidding or slipping. In this case, $\omega_i \approx v/r$ and $F_{xi} \approx T_{mi}/r$ hold. Accordingly, the longitudinal force of the vehicle is actualized by the wheel torques, including motor torques and hydraulic torques.

$$F_{veh} = \sum_{i=1}^{4} F_{xi} \approx \sum_{i=1}^{4} (T_{mi} - T_{hi})/r \tag{4}$$

$$T_{veh} = F_{veh} r \approx \sum_{i=1}^{4} (T_{mi} - T_{hi}) \tag{5}$$

where $T_{mi} \geq 0$ and $T_{hi} = 0$ for driving cases, whereas $T_{mi} \leq 0$ and $T_{hi} \geq 0$ for braking cases.

Take driving control with $F^*_{veh} > 0$ for instance to study the energy efficiency optimization. The desired vehicle total torque is defined as

$$T^*_{veh} = \min\left(F^*_{veh} r, \sum_{i=1}^{4} (T_{mmax}(\omega_i))\right).$$

Because the battery power should be minimized to reduce the energy consumption, we select $T^*_{mi} > 0$ and the energy efficiency optimization problem can be written as

$$\begin{aligned} \min_{T_{mi}^*} \; & J_1 = \sum_{i=1}^{4} \frac{\omega_i \cdot T^*_{mi}}{\eta_{di}(\omega_i, T^*_{mi})} \\ \text{s.t.} \; & \sum_{i=1}^{4} T^*_{mi} = T^*_{veh} \\ & 0 \leq T^*_{m,i} \leq T_{mmax}(\omega_i) \end{aligned} \tag{6}$$

Since no obvious wheel slip exists under a stable driving maneuver, it can be approximately obtained that $\omega_i \approx v/r$. Besides, the four in-wheel motors are the same, so the energy optimization problem can be studied in half part of the vehicle, i.e., $T^*_{m1} = T^*_{m2}$, $T^*_{m3} = T^*_{m4}$, and $T^*_{veh} = \min(F^*_{veh} r, 4\, T_{mmax}(v))$. Then, by considering $v$ as a slow-varying parameter, the optimization problem can be simplified as

$$\begin{aligned} \min_{T_{m1}^*} \; & J_1' = \frac{v \cdot T^*_{m1}}{\eta_{d1}(v, T^*_{m1})} + \frac{v \cdot (T^*_{veh}/2 - T^*_{m1})}{\eta_{d3}(v, (T^*_{veh}/2 - T^*_{m1}))} \\ \text{s.t.} \; & 0 \leq T^*_{m1} \leq T_{mmax}(v) \end{aligned} \tag{7}$$

where the efficiency is defined as $\eta_{di} = (T_{mi}\omega_i)/(UI)$ to describe how much battery power is transferred to the

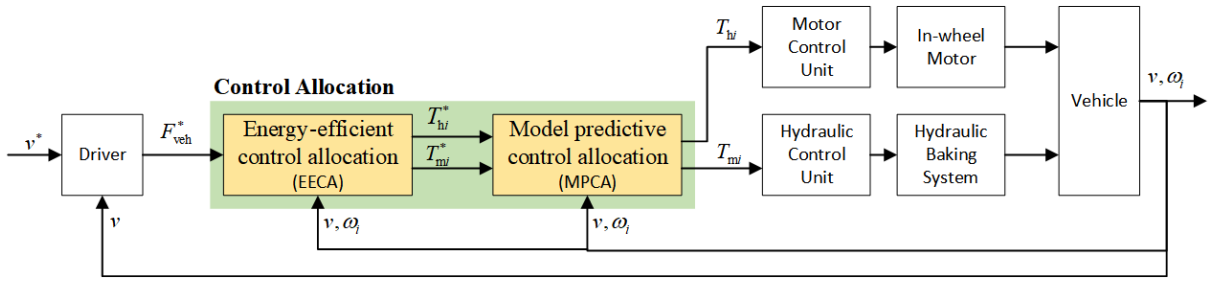


**FIGURE 3.** Control system framework.

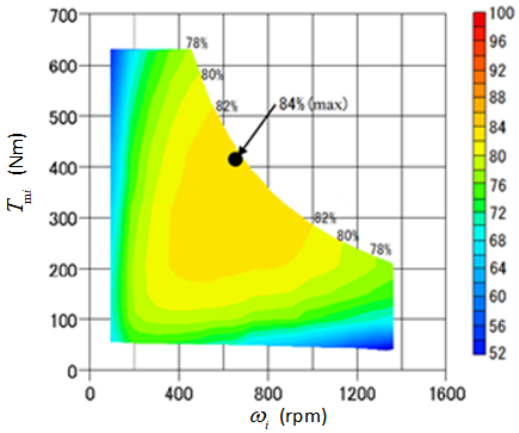


**FIGURE 4.** Battery to motor efficiency characteristics of the mounted actuating module.

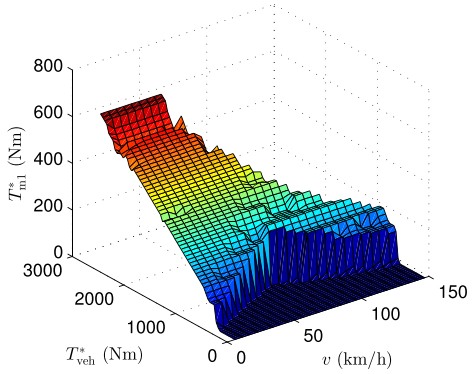


**FIGURE 5.** Energy efficiency optimization solution for $T^*_{m1}$ respect to various $T^*_{veh}$ and $v$.

motor output power. It is usually written as $\eta_{di}(\omega_i, T_{mi})$ and described as a MAP, as shown in Figure 4.

As the efficiency is highly nonlinear and always described as a MAP, it is difficult to get an analytic solution. Hence, a numerical method is used. At each instantaneous time, $v$ is assumed to be a constant. So $T^*_{m1}$ is the only variable for optimization. By setting various $T^*_{m1}$ for some typical vehicle speed to complete an ergodic process, we can get rid of local solutions and select a tendentious one when they are not unique. In this way, we can get an optimal control allocation for various requirement $T^*_{veh}$ under various vehicle speed, which is described as a map shown in Figure 5. For low $T^*_{veh}$, the two-wheel-driving mode is preferred. And the rear wheels are chosen as driving wheels so as to provide higher maximum adhesion force. In application, the optimal target torque $T^*_{m1}$ will be calculated on line using look-up table and interpolation, and then $T^*_{m3} = T^*_{veh}/2 - T^*_{m1}$ is also obtained.

As for the braking case with $F^*_{veh} < 0$, The desired total braking torque is $T^*_{veh} = F^*_{veh} r$, while the desired total torque for generative braking is defined as $T^*_{rb} = \max(F^*_{veh} r, -4\ T_{mmax}(v))$. The total power of the battery should be maximized to recover as much energy as possible from the in-wheel motors at a given braking torque. Similar to the driving case, the optimization solution for regenerative braking can be obtained by

$$\begin{aligned} \min_{T_{m1}^*} \ & J_1' = v \cdot T^*_{m1} \cdot \eta_{b1}(v, T^*_{m1}) \\ & \quad + v \cdot (T^*_{veh}/2 - T^*_{m1}) \cdot \eta_{b3}(v, (T^*_{veh}/2 - T^*_{m1})) \\ \text{s.t.} \ & -T_{mmax}(v) \le T^*_{m1} \le 0. \end{aligned} \tag{8}$$

Besides, hydraulic braking is needed to provide sufficient torque for low speed or strong braking. The hydraulic braking is activated by an active braking system such as Bosch iBooster, and the hydraulic torques for front and rear wheels are distributed with a constant ratio $\beta$

$$\begin{cases} T^*_{h1} = T^*_{h2} = \beta((T^*_{m1} + T^*_{m3}) - T^*_{veh}/2) \\ T^*_{h3} = T^*_{h4} = (1-\beta)((T^*_{m1} + T^*_{m3}) - T^*_{veh}/2) \end{cases} \tag{9}$$

To sum up, a reference solution is obtained for the wheel torque distribution with the purpose for energy efficiency, written as

$$u^* = [T^*_{m1}, T^*_{m2}, T^*_{m3}, T^*_{m4}, T^*_{h1}, T^*_{h2}, T^*_{h3}, T^*_{h4}]^{\mathrm{T}} \tag{10}$$

### B. MODEL PREDICTIVE CONTROL ALLOCATION (MPCA)

The energy-saving objective can be achieved in most cases using the previous method, but its application is limited to the stable driving cases. For complex conditions such as driving on a low adhesion road, the wheels might skid or slip. To ensure the vehicle stability, the friction constraints should be taken into account to reallocate the control torque to

avoid the wheels from skidding or locking. In this section, a model predictive controller is designed for torque reallocation. Firstly, the control-oriented model is given based on vehicle dynamics. Then the cost function and constrains are established for the purpose of braking stability and energy optimization. Finally, the solution and application of the method are discussed.

### 1) VEHICLE MODEL

Various estimation methods or measurement approaches such as GPS are developed and applied in practice, the vehicle speed is considered to be obtained in real-time, so the wheel slip dynamics are utilized for the controller design. From (1)-(3), the motor torques and hydraulic torques for each wheel can be regulated independently. The system states and control variables are defined as $x = [\lambda_1, \lambda_2, \lambda_3, \lambda_4]^{\mathrm{T}}$, and $u = [T_{\mathrm{m1}}, T_{\mathrm{m2}}, T_{\mathrm{m3}}, T_{\mathrm{m4}}, T_{\mathrm{h1}}, T_{\mathrm{h2}}, T_{\mathrm{h3}}, T_{\mathrm{h4}}]^{\mathrm{T}}$.

Combining the four wheel-slip-dynamics models, the state equation can be described as follows

$$\dot{x} = f(x) + Bu \tag{11}$$

where $f(x) = -\frac{r^2}{vJ_{\mathrm{w}}}\mathrm{diag}\{[f(F_{\mathrm{z1}}, \lambda_1), f(F_{\mathrm{z2}}, \lambda_2), f(F_{\mathrm{z3}}, \lambda_3), f(F_{\mathrm{z4}}, \lambda_4)]\}$, $B = \frac{r}{vJ_{\mathrm{w}}}[-I_4, I_4]$.

### 2) COST FUNCTION

The cost function is designed to satisfy several demands: to carry out the pre-allocated control, to satisfy the wheel slip constraints, and also to respond to the desired longitudinal force.

The primary objective is the energy optimization. Since this issue has been solved using off-line optimization and the on-line look-up table in the previous section, the objective is accomplished by including the control tracking error square from current time $t$ to $t + pT_s$ in the cost function

$$J_{21} = \int_t^{t+pT_s} \|u - u^*\|^2 d\tau \tag{12}$$

Moreover, as illustrated in Figure 2, the wheel slip directly reflects tire friction saturation and the vehicle stability. Soft constraints $x_i \in [-\lambda_{\max}, \lambda_{\max}]$ are imposed on the wheel slip ratios to achieve stable operating conditions, which is described as an additional penalty term in the cost function.

$$J_{22} = \int_t^{t+pT_s} \|E_i(\tau)\|^2 d\tau \tag{13}$$

where the penalty function $E_i(\tau)$ is formulated as

$$E_i = \begin{cases} (x_i - \lambda_{\max})/\lambda_{\max}, & x_i > \lambda_{\max} \\ 0, & -\lambda_{\max} \le x_i \le \lambda_{\max} \\ (x_i + \lambda_{\max})/\lambda_{\max}, & x_i < -\lambda_{\max} \end{cases} \tag{14}$$

Another objective is to meet the requirement of the driver's driving or braking command. This can be met naturally when all wheels are stable. However, if one or two wheels tends to skid or slip due to a spot of low adhesion road, (12) cannot be minimized since (13) takes effect. Noting that the vehicle total torque can also be satisfied by transferring some torque to other wheels, the third cost function is to make the sum of the total torque error square as small as possible

$$J_{23} = \int_t^{t+pT_s} \|B_{\mathrm{veh}}u - T^*_{\mathrm{veh}}\|^2 d\tau \tag{15}$$

where $B_{\mathrm{veh}} = [1, 1, 1, 1, -1, -1, -1, -1]$.

These three objectives are accounted for by the following terms in the integral cost function, and a mixed-optimization formulation is obtained.

$$\begin{aligned} &\min_u \ J_2 = q_1 J_{21} + q_2 J_{22} + q_3 J_{23} \\ &\text{s.t. } \dot{x} = f(x) + Bu \\ &\begin{cases} 0 \le T_{\mathrm{m}i} \le T_{\mathrm{mmax}}(v), T_{\mathrm{h}i} = 0, & \text{for driving} \\ \text{or } -T_{\mathrm{mmax}}(v) \le T_{\mathrm{m}i} \le 0, T_{\mathrm{h}i} \ge 0, & \text{for braking} \end{cases} \end{aligned} \tag{16}$$

where $q_1$, $q_2$, and $q_3$ are weighting weight coefficients.

The system (16) is dependent on the vehicle speed, but the vehicle dynamics is relatively slow when comparing with wheel dynamics due to the large mass. Hence, the vehicle speed is assumed to be constant for the duration of the prediction horizon, and then updated in each sampling step.

### 3) MODEL PREDICTIVE CONTROL LAW

From (16), It comes to a nonlinear model predictive control (NMPC) issue. According to the current measurement information, the finite horizon optimization problems is solved online at each sampling time, and then this procedure is repeated at next sampling time on the basis of the new measurements. In this research, Matlab function fmincon in optimization tool box is used for simulation validation. Although the method is not applied to the experimental vehicle, it is still quite promising for practical application. Firstly, many low-computation optimization tools have been put in use, e.g., MPC with PSO in [31] and GRAMPC with a recently published gradient-based algorithm in [20]. Moreover, the calculation ability of the electronic control unit has been highly improved. Putting the controller into practice will be our work in the next.

**TABLE 1. Parameters of the simulation mode and controller.**

| Variable | Value | Unit |
|---|---|---|
| $M$ | 1300 | kg |
| $r$ | 0.28 | m |
| $J_{\mathrm{w}}$ | 2 | $\mathrm{kg \cdot m/s^2}$ |
| $\lambda_{\max}$ | 0.05 | – |
| $p$ | 2 | – |
| $q_1$ | 1 | – |
| $q_2$ | $3 \times 10^5 \times v$ | – |
| $q_3$ | 10 | – |

## IV. SIMULATION RESULTS

The proposed control allocation strategy is validated with simulations on a professional software veDYNA, which is

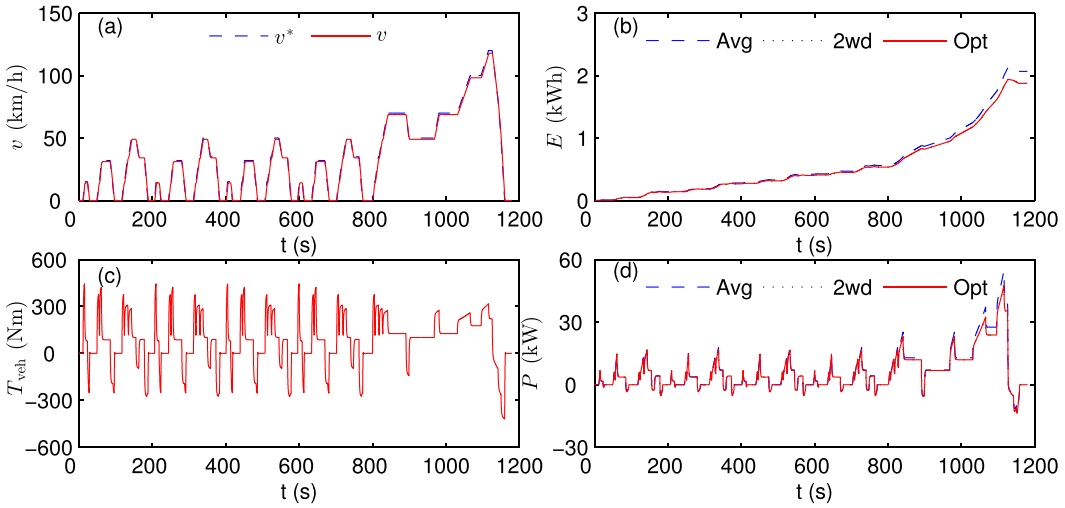


**FIGURE 6.** NEDC test result for energy consumption.

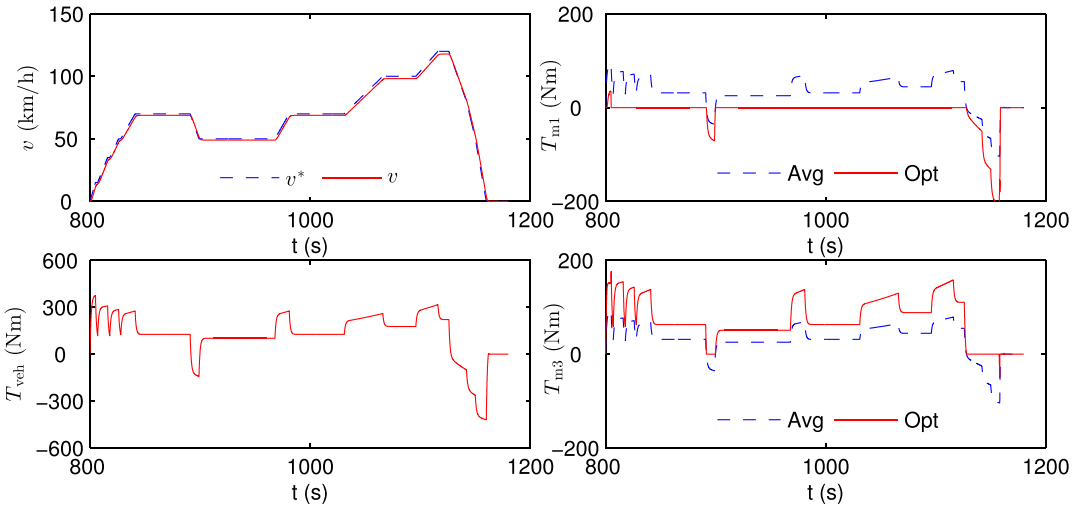


**FIGURE 7.** NEDC test result for control allocation.

widely used in BMW and other institutes [30]. It mainly includes a high-fidelity vehicle dynamics model, a driver module, and also a road setting. Apart from the traditional vehicle dynamics, the veDYNA model also explicitly considers four in-wheel motors modules, a battery pack module, so that it is capable of simulating the experimental vehicle motion in 3-D environments. Some parameters of the simulation model and the controller are given in Table 1, with the sample time set as $T_s = 0.01$s. Herein, $q_2$ is selected to be dependent on $v$ in practical application to avoid from serious oscillation under low speed, noting that the wheel slip dynamics are related with the vehicle speed. In the following, several typical cases are simulated to verify the effectiveness of the developed controller, i.e., a NEDC (New European Driving Cycle) test for energy efficiency evaluation on high adhesion road, an acceleration and deceleration test for vehicle stability validation on low adhesion road, and an acceleration test for dynamic torque distribution on $\mu$-split road.

### A. NEDC TEST

Firstly, a NEDC test is conducted to illustrate the efficiency of the proposed strategy, as shown in Figure 6. Figure 6 (a) shows that the actual vehicle speed $v$ can well track the NEDC reference curve $v^*$. From Figure 6 (c), the vehicle torque $T_{\text{veh}}$ is not so high, implying that the vehicle is working in stable status. It means that the penalty term on the wheel slip does not work, and the final controller output $u$ is the same as $u^*$ determined by EECA. To better show the effectiveness of the proposed control allocation method (Opt for short), the equally distributed torque method (Avg for short) and the

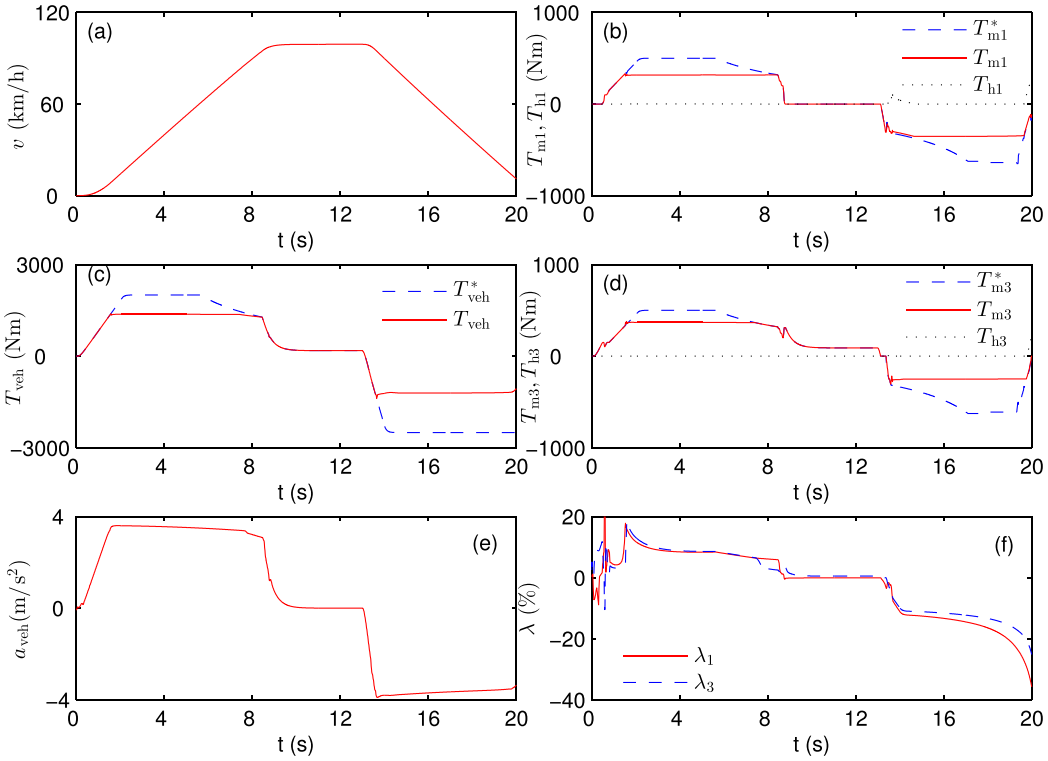


**FIGURE 8.** Low adhesion road test result for control allocation.

two-wheel-driving method (2wd for short) are also simulated and compared. Both the total power $P$ and $E$ energy are given in Figure 6 (b) and (d). It can be seen that the proposed method is consistent with the two-wheel-driving method, and can save about 5% energy than the equally distributed torque method. That is because the motor efficiency is low for a small torque, and only the front two or rear two motors are actuated and work at a higher efficiency range, as illustrated in Figure 5. Specifically, Figure 7 shows the wheel torques for high speed from 800s to 1200s. For the proposed method, the rear wheels will output positive motor torque $T_{m3}$ for driving process while the front wheels output negative torque $T_{m1}$ for braking process, which is consistent with the vehicle load transfer. This simulation illustrates that the proposed law is beneficial for energy saving, especially for driving on highways.

### B. LOW ADHESION ROAD TEST

Secondly, a low adhesion road test is carried out to validate the controller's ability to keep the vehicle stability under critical conditions. There are three phases in this test: (1) a sharp acceleration from 0s to 9s; (2) cruise around 100km/h from 9s to 13s; (3) a panic brake from 13s to the end. The simulation results are illustrated in Figure 8. Firstly, the acceleration process is discussed. From Figure 8 (c), (b), (d), the EECA module commands $T^*_{m1} = T^*_{m3} = 500$Nm to meet the driver's driving requirement (2000Nm), but it is markedly greater than the torque provide by the road-tire friction. Then the MPCA module limits the actual motor torques $T_{m1}$ and $T_{m3}$ at around 300Nm, so that the wheel slip ratios $\lambda_i$ are constrained under 20% as shown in Figure 8 (f). The driver's vehicle torque $T^*_{veh}$ is limited to ensure the vehicle stability. Secondly, when cruising, the control allocation transits from the equally distributed torque mode and the two-wheel-driving mode, in order to improve the energy saving. Finally, the braking process is similar to the acceleration process, with only a few differences. From Figure 8 (b), (d), since the motor torques are limited by the maximum power, the hydraulic braking torque is actuated for supplement. Besides, since the regenerative braking is not available for low vehicle speed, the hydraulic braking would also supply. Furthermore, due to the selected weighting coefficient $q_2$ get lower as the vehicle speed decreases, the wheel slip ratios are a bit higher for speed less than 20km/h. In this way, no serious oscillation occurs, and there is no obvious decline in braking performance. This simulation illustrates that the proposed law can ensure the vehicle stability even under critical conditions such as on the low adhesion road.

### C. $\mu$-SPLIT ROAD TEST

Finally, a $\mu$-split road test is performed to verify the controller's ability to dynamically distribute the wheel torques in the transitional condition between the stable and critical cases. The adhesion coefficient is low on the left and high on the right. Figure 9 shows a result for acceleration test on the $\mu$-split road. The total desired torque of the vehicle $T^*_{veh}$ is plot in Figure 9 (c). Figure 9 (b) and (d) show the expected torque of the EECA module for one front wheel

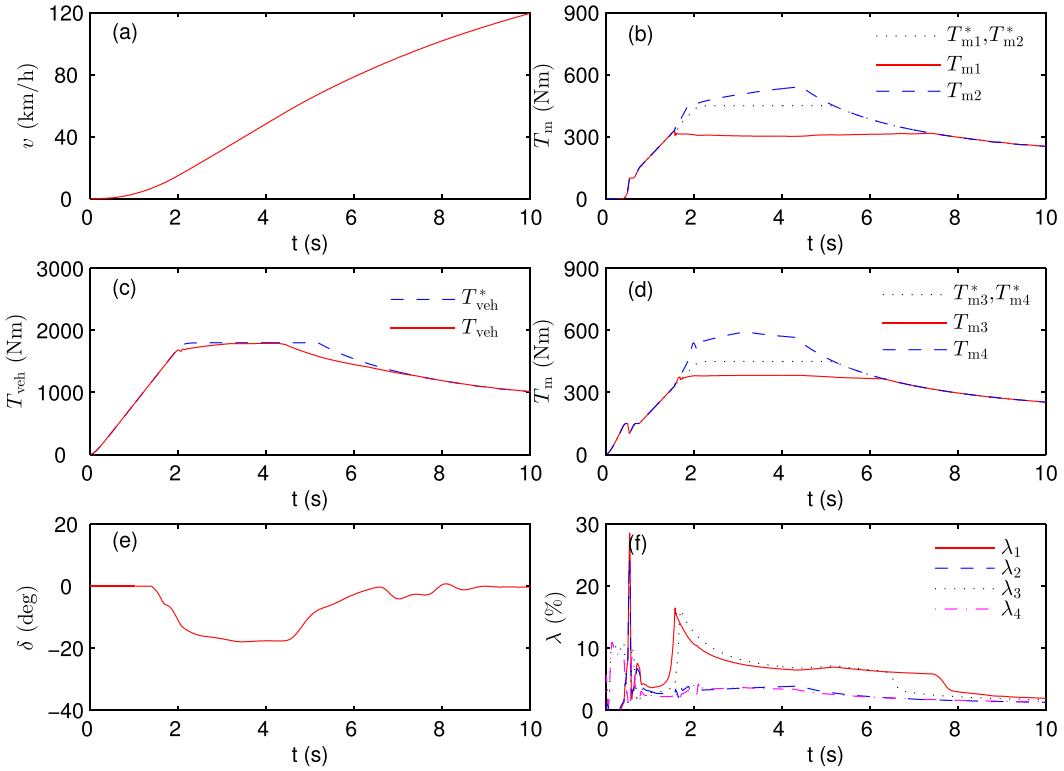


**FIGURE 9.** $\mu$-split road test result for control allocation.

$T^*_{\rm m1}$ and one rear wheel $T^*_{\rm m3}$. Clearly, the left two wheels would tend to skid due to the low adhesion under so excessive torque. Hence, although the EECA module commands the same torques for the left and right wheels, the actual torques after the MPCA module become different. For the left side, the torques $T_{\rm m1}$ and $T_{\rm m3}$ are reduced to avoid the wheels from skidding, while the right wheels increase the torques $T_{\rm m2}$ and $T_{\rm m4}$. In this way, the vehicle total torque $T_{\rm veh}$ can also be satisfied by dynamically distribution, and all the wheel slip ratios $\lambda_i$ are kept in the stable region. From Figure 9 (a), it is clear that a good acceleration is obtained. Besides, the driver needs to take a steer $\delta$ to keep the vehicle in its lane, which is shown in Figure 9 (e). In the existing research, even though only one-side wheels slip, the wheel slip controller would be actuated to replace with the energy optimal controller, resulting in unnecessary controller switching or performance loss. This simulation illustrates that the proposed law is helpful to enhance the vehicle acceleration capability under complicated transitional conditions such as on the $\mu$-split road.

## V. CONCLUSION

To trade off energy optimization and driving stability in actual complicated conditions, a multi-objective optimal control allocation problem is presented, and a two-step optimal control allocation law is developed. By combining the energy efficiency control allocation and model predictive control allocation, the approach can improve the energy saving in most cases, keep the vehicle stability in critical conditions, and also enhance the vehicle acceleration/deceleration capability under some transitional conditions. It acts as a self-adapting controller to highlight energy or stability according to the actual situation. Simulations are performed via a professional vehicle dynamics software to verify the controller's practicability and effectiveness. In the next, both battery characteristic and actuator failures will be taken into account to improve the performance, and we will also work on putting it into practical application on the experimental vehicle.

## APPENDCES

Nomenclature list:

| | |
|---|---|
| $a_{\rm veh}$ | longitudinal acceleration of the vehicle (m/s$^2$) ; |
| $E$ | total consumed energy of the vehicle (kW · h); |
| $F_{\rm veh}$ | total longitudinal force of the vehicle for driving or braking (N); |
| $F_{{\rm x}i}$ | longitudinal tire-road friction force of the i-th wheel (Nm); |
| $F_{{\rm z}i}$ | normal force supported by the i-th wheel (Nm); |
| $J_{\rm w}$ | wheel rotation inertia (kg · m/s$^2$); |
| $I$ | battery current (A); |
| $M$ | vehicle mass (m); |
| $P$ | total power of the vehicle (kW); |
| $r$ | effective rolling radius of the wheel (m); |
| $T_{{\rm m}i}$ | torque provided by the i-th in-wheel motor actuating module (Nm), positive for driving and negative for regenerative braking; |

| | |
|---|---|
| $T_{\mathrm{mmax}}$ | maximum torque of the in-wheel motor actuating module (Nm), which is dependent on wheel rotational speed according to the motor's external characteristic; |
| $T_{\mathrm{hi}}$ | hydraulic braking torque of the i-th wheel (Nm); |
| $T_{\mathrm{veh}}$ | vehicle total torque on wheels for driving or braking (Nm); |
| $U$ | battery voltage (V); |
| $v$ | longitudinal velocity of the vehicle (m/s); |
| $\delta$ | steering wheel angle (deg); |
| $\eta_{\mathrm{di}}$ | driving efficiency of the i-th in-wheel motor actuating module (%); |
| $\eta_{\mathrm{bi}}$ | energy recovery efficiency of the i-th in-wheel motor actuating module (%); |
| $\lambda_i$ | wheel slip ratio of the i-th wheel (%); |
| $\eta_{\mathrm{max}}$ | constraint on wheel slip ratio (%); |
| $\omega_i$ | wheel rotational speed of i-th wheel (rad/s); |

where $i = 1, 2, 3, 4$ denote front left, front right, rear left and rear right, respectively. Besides, variable with superscript * denotes its desired value.

## REFERENCES

[1] S. F. Tie and C. W. Tan, "A review of energy sources and energy management system in electric vehicles," *Renew. Sustain. Energy Rev.*, vol. 20, pp. 82–102, Apr. 2013.

[2] C. C. Chan, A. Bouscayrol, and K. Chen, "Electric, hybrid, and fuel-cell vehicles: Architectures and modeling," *IEEE Trans. Veh. Technol.*, vol. 59, no. 2, pp. 589–598, Feb. 2010.

[3] K. Maeda, Y. Hori, and H. Fujimoto, "Four-wheel driving-force distribution method for instantaneous or split slippery roads for electric vehicle with in-wheel motors," in *Proc. IEEE Int. Workshop Adv. Motion Control (AMC)*, Sarajevo, Bosnia-Herzegovina, Mar. 2012, pp. 1–6.

[4] K. Nam, Y. Hori, and C. Lee, "Wheel slip control for improving traction-ability and energy efficiency of a personal electric vehicle," *Energies*, vol. 8, no. 7, pp. 6820–6840, 2015.

[5] R. de Castro, R. E. Araujo, M. Tanelli, S. Savaresi, and D. Freitas, "Torque blending and wheel slip control in EVs with in-wheel motors," *Vehicle Syst. Dyn., Int. J. Vehicle Mech. Mobility*, vol. 50, no. 1, pp. 71–94, Jul. 2012.

[6] N. Mutoh, "Driving and braking torque distribution methods for front- and rear-wheel-independent drive-type electric vehicles on roads with low friction coefficient," *IEEE Trans. Ind. Electron.*, vol. 59, no. 10, pp. 3919–3933, Oct. 2012.

[7] R. Wang, H. Zhang, and J. Wang, "Linear parameter-varying controller design for four-wheel independently actuated electric ground vehicles with active steering systems," *IEEE Trans. Control Syst. Technol.*, vol. 22, no. 4, pp. 1281–1296, Jul. 2014.

[8] R. de Castro, M. Tanelli, R. E. Araújo, and S. M. Savaresi, "Design of safety-oriented control allocation strategies for overactuated electric vehicles," *Veh. Syst. Dyn.*, vol. 52, no. 8, pp. 1017–1046, 2014.

[9] B. Shyrokau, D. Wang, D. Savitski, and V. Ivanov, "Vehicle dynamics control with energy recuperation based on control allocation for independent wheel motors and brake system," *Int. J. Powertrains*, vol. 2, nos. 2–3, pp. 153–181, 2013.

[10] H. Fujimoto, J. Saito, K. Handa, and S. Egami, "Range extension control system for electric vehicle based on searching algorithm of optimal front and rear driving force distribution," in *Proc. Annu. Conf. IEEE Ind. Electron. Soc.*, Montreal, QC, Canada, Oct. 2012, pp. 4264–4269.

[11] J. Brembeck and P. Ritzer, "Energy optimal control of an over actuated robotic electric vehicle using enhanced control allocation approaches," in *Proc. Intell. Veh. Symp.*, Alcala de Henares, Spain, Jun. 2012, pp. 322–327.

[12] R. Wang, Y. Chen, D. Feng, X. Huang, and J. Wang, "Development and performance characterization of an electric ground vehicle with independently actuated in-wheel motors," *J. Power Sour.*, vol. 196, no. 8, pp. 3962–3971, 2011.

[13] Y. Chen and J. Wang, "Fast and global optimal energy-efficient control allocation with applications to over-actuated electric ground vehicles," *IEEE Trans. Control Syst. Technol.*, vol. 20, no. 5, pp. 1202–1211, Sep. 2012.

[14] Y. Chen and J. Wang, "Adaptive energy-efficient control allocation for planar motion control of over-actuated electric ground vehicles," *IEEE Trans. Control Syst. Technol.*, vol. 22, no. 4, pp. 1362–1373, Jul. 2014.

[15] Y. Chen and J. Wang, "Design and experimental evaluations on energy efficient control allocation methods for overactuated electric vehicles: Longitudinal motion case," *IEEE/ASME Trans. Mechatronics*, vol. 19, no. 2, pp. 538–548, Apr. 2014.

[16] Y.-P. Yang, Y.-C. Shih, and J.-M. Chen, "Real-time torque distribution strategy for an electric vehicle with multiple traction motors by particle swarm optimization," in *Proc. Autom. Control Conf.*, Nantou, Taiwan, Dec. 2013, pp. 233–238.

[17] K. Ramakrishnan, M. Gobbi, and G. Mastinu, "Multi-objective optimization of in-wheel motor powertrain and validation using vehicle simulator," in *Proc. Int. Conf. Ecol. Veh. Renew. Energies (EVER)*, Monte Carlo, Monaco, Mar./Apr. 2015, pp. 1–9.

[18] S. Koehler, A. Viehl, O. Bringmann, and W. Rosenstiel, "Energy-efficient torque distribution for axle-individually propelled electric vehicles," in *Proc. IEEE Intell. Veh. Symp.*, Dearborn, MI, USA, Jun. 2014, pp. 1109–1114.

[19] W. Xu, H. Zhao, B. Ren, and H. Chen, "A regenerative braking control strategy for electric vehicle with four in-wheel motors," in *Proc. Chin. Control Conf. (CCC)*, Chengdu, China, Jul. 2016, pp. 8671–8676.

[20] T. Bächle, K. Graichen, M. Buchholz, and K. Dietmayer, "Slip-constrained model predictive control allocation for an all-wheel driven electric vehicle," *IFAC Proceedings Volumes*, vol. 47, no. 3, pp. 12042–12047, 2014.

[21] T. Bächle, K. Graichen, M. Buchholz, and K. Dietmayer, "Vehicle dynamics control in challenging driving situations using nonlinear model predictive control allocation," in *Proc. IEEE Conf. Control Appl. (CCA)*, Juan Les Antibes, France, Oct. 2014, pp. 346–351.

[22] T. Bächle, K. Graichen, M. Buchholz, and K. Dietmayer, "Model predictive control allocation in electric vehicle drive trains," *IFAC-PapersOnLine*, vol. 48, no. 15, pp. 335–340, 2015.

[23] X. Huang and J. Wang, "Model predictive regenerative braking control for lightweight electric vehicles with in-wheel motors," *Proc. Inst. Mech. Eng., D, J. Automobile Eng.*, vol. 226, no. 9, pp. 1220–1232, 2012.

[24] C. Satzger, R. de Castro, and T. Bünte, "A model predictive control allocation approach to hybrid braking of electric vehicles," in *Proc. IEEE Intell. Veh. Symp.*, Dearborn, MI, USA, Jun. 2014, pp. 286–292.

[25] G. Xu, K. Xu, C. Zheng, X. Zhang, and T. Zahid, "Fully electrified regenerative braking control for deep energy recovery and maintaining safety of electric vehicles," *IEEE Trans. Veh. Technol.*, vol. 65, no. 3, pp. 1186–1198, Mar. 2016.

[26] L. Zhang, L. Yu, N. Pan, Y. Zhang, and J. Song, "Cooperative control of regenerative braking and friction braking in the transient process of anti-lock braking activation in electric vehicles," *Proc. Inst. Mech. Eng. D, J. Automobile Eng.*, vol. 230, no. 11, pp. 1459–1476, 2016.

[27] H. Yeo and H. Kim, "Hardware-in-the-loop simulation of regenerative braking for a hybrid electric vehicle," *Proc. Inst. Mech. Eng. D, J. Automobile Eng.*, vol. 216, no. 11, pp. 855–864, 2002.

[28] M. Soga, M. Shimada, J.-I. Sakamoto, and A. Otomo, "Development of vehicle dynamics management system for hybrid vehicles: ECB system for improved environmental and vehicle dynamic performance," *JSAE Rev.*, vol. 23, no. 4, pp. 459–464, 2002.

[29] W. Sun, H. Pan, and H. Gao, "Filter-based adaptive vibration control for active vehicle suspensions with electrohydraulic actuators," *IEEE Trans. Veh. Technol.*, vol. 65, no. 6, pp. 4619–4626, Jun. 2016.

[30] H. Jing, Z. Liu, and H. Chen, "A switched control strategy for antilock braking system with on/off valves," *IEEE Trans. Veh. Technol.*, vol. 60, no. 4, pp. 1470–1484, May 2011.

[31] B. Ren, H. Chen, H. Zhao, and L. Yuan, "MPC-based yaw stability control in in-wheel-motored EV via active front steering and motor torque distribution," *Mechatronics*, vol. 38, pp. 103–114, Sep. 2015.

**HOUHUA JING** received the B.S. and Ph.D. degrees from the Harbin Institute of Technology, Harbin, China, in 2005 and 2012, respectively. Since 2012, he has been with the Harbin Institute of Technology. His research interests include automotive control and optimal control.

**FENGJIAO JIA** received the B.S. degree from Shandong University at Weihai, Weihai, China, in 2012, and the M.S. degree from the Harbin Institute of Technology, Harbin, China, in 2014, where she is currently pursuing the Ph.D. degree with the Department of Control Science and Engineering. Her research interests include vehicle dynamics and control.

**ZHIYUAN LIU** (M'11) received the B.S. degree from the Zhejiang University of Technology, Hangzhou, China, in 1982, and the Ph.D. degree in control science and engineering from the Harbin Institute of Technology, Harbin, China, in 1992. From 1992 to 1994, he was a Post-Doctoral Fellow with the Department of Mechanical Engineering, Harbin Institute of Technology, where he has been with the Department of Control Science and Engineering since 1994 and he became a Professor in 1999. His research interests include automotive electronic control, robotics, robust control, and model predictive control.